Biosensors and Bioelectronics 40 (2013) 17–23

Contents lists available at SciVerse ScienceDirect

Biosensors and Bioelectronics

journal homepage: www.elsevier.com/locate/bios

Detection of vimentin serine phosphorylation by multicolor Quenchbodies

Hee-Jin Jeong [a], Yuki Ohmuro-Matsuyama [a], Hiroyuki Ohashi [a], Fuyuki Ohsawa [a], Yoshiro Tatsu [b], Masaki Inagaki [c,*], Hiroshi Ueda [a,**]

[a] Department of Chemistry and Biotechnology, School of Engineering, The University of Tokyo, 7-3-1 Hongo, Bunkyo-ku, Tokyo 113-8656, Japan
[b] National Institute of Advanced Industrial Science and Technology, Midorigaoka, Ikeda, Osaka 563-8577, Japan
[c] Division of Biochemistry, Aichi Cancer Center Research Institute, Kanokoden, Chikusa-ku, Nagoya 464-8681, Japan

ARTICLE INFO

Available online 23 June 2012

Keywords:
Quenchbody
Vimentin
Protein phosphorylation
Fluorescence quenching
Single chain antibody

ABSTRACT

Protein phosphorylation is a key event in intracellular signal transduction, and fluorescent biosensor for the specific phosphorylation event in a target protein is considered highly useful as a tool of cellular biology and drug screening. Vimentin, the most abundant intermediate filament protein, is phosphorylated at its specific serine (Ser) residues in a cell cycle dependent manner. Its structural and functional characteristics are modified by the phosphorylation, which affects biological properties of the cell. Here we present the detection of the vimentin Ser71 phosphorylation (PS71) and the vimentin Ser82 phosphorylation (PS82) using a novel fluorescent biosensor Quenchbody, which works on the principle of antigen-dependent removal of a quenching effect by intrinsic tryptophan residues on a carboxytetramethylrhodamine (TAMRA) dye incorporated at the N-terminal region of single chain antibody variable region. First, we found that rhodamine 6G (R6G)-labeled Quenchbody shows superior response than TAMRA-labeled one. Next, we made several Quenchbodies to detect PS71 and PS82. After optimization of reaction conditions, the fluorescence intensity of V_H-V_L type PS71 Quenchbody labeled with R6G at two positions was increased to 4.0-fold in an antigen dependent manner. Furthermore, the fluorescence intensity of doubly R6G-labeled V_L-V_H type PS82 Quenchbody was increased to 6.7-fold immediately after adding antigen peptide, also suggesting deeper quenching due to H-dimer formation between the dyes. Due to its simplicity, the Quenchbody-based phosphorylation biosensors will be widely applicable to in vitro diagnostics, drug screening and imaging in a rapid, simple and high-sensitive manner.

1. Introduction

Protein functions are complexly modulated by phosphorylation in both prokaryotic and eukaryotic organisms. The protein phosphorylation has a significant role in a wide range of cellular processes and is involved in intracellular signal transduction, which distributes signals to various parts of the cell (Graves and Krebs, 1999; Marks, 2001; Mundy and Schneitz, 2002; Sawyer et al., 2005). Therefore, protein phosphorylation is an important recognition marker for the regulation of cellular functions. Until now, a fluorescent biosensor, whose fluorescence intensity is increased by its binding to a target protein, has been used as a powerful tool for protein characterization, e.g. for the detection of the phosphorylated protein, and thus considered highly useful for cellular biology, drug screening and diagnosis of diseases (Brune et al., 2001; Cotton and Muir, 2000; Holford et al., 2012; Kawai et al., 2004; Lawrence and Wang, 2007).

Vimentin, the most abundant intermediate filament protein, is phosphorylated at its serine (Ser) residues in a cell cycle dependent manner (Aziz et al., 2010; Izawa and Inagaki, 2006; Minin and Moldaver, 2008). The phosphorylation causes degradation and disassembly of the protein, and subsequently the conformation of the protein is changed during the cell division, which affects biological properties of the cell (Inagaki et al., 1987; Ivaska et al., 2007; Pittenger et al., 2008; Sihag et al., 2007). Therefore, it is considered important to detect this vimentin Ser phosphorylation.

Several methods including a kinase assay and an immunoprecipitation assay have been used for detecting the vimentin phosphorylation *in vivo* (Chang et al., 2012; Takai et al., 1996; Thaiparambil et al., 1989). These assays enabled the imaging of the vimentin phosphorylation in the fixed cells as well as the measurement of the structural change in phosphorylated vimentin. However, all these methods require several laborious and technically demanding steps to prepare the samples. Bouamrani et al. (2010) and Pittenger et al. (2008) studied the role of vimentin phosphorylation by mass spectrometry (MS), which

* Corresponding author. Tel.: +81 52 762 6111; fax: +81 52 763 5233.
** Corresponding author. Tel./fax: +81 3 5841 7362.
E-mail addresses: minagaki@aichi-cc.jp (M. Inagaki), hueda@chembio.t.u-tokyo.ac.jp (H. Ueda).

0956-5663/$ - see front matter © 2012 Elsevier B.V. All rights reserved.
http://dx.doi.org/10.1016/j.bios.2012.06.030

can identify phosphopeptides with high resolution. However, while they found major peaks of phosphorylated vimentin sample, distinction of weaker signals from lower abundant phosphopeptides and high background of abundant non-phosphorylated peptides make identification of phosphorylation marker difficult. Moreover, site-specific and quantitative detection of phosphorylation is hard to achieve with the MS-based method. Aziz et al. (2010) and Pittenger et al. (2008) established a site-directed spin labeling and electron paramagnetic resonance method for the detection of vimentin phosphorylation and demonstrated the phosphorylation–induced disassembly of vimentin. However, since the phosphorylation was identified in multiphosphorylated forms, additional methods are required to identify the specific phosphorylated amino acid residues in the protein. To overcome this problem, further investigations have enabled the site-specific detection of vimentin Ser phosphorylation by Western blot analysis using anti-vimentin Ser phosphorylation antibodies (Chang et al., 2012; Goto and Inagaki, 2007; Lee et al., 2011; Thaiparambil et al., 1989). However, the measured levels of phosphoproteins detected by Western blot analysis are readily affected by many experimental errors such as that of gel loading, fluctuations in non-specific binding and background staining, and inaccuracy of band intensity-based quantitation. Also, despite its sensitivity and linearity, radioisotope-based kinase assays need special care, and they are not readily performed in normal biochemical laboratories (Lee et al., 2011).

To this end, we recently showed the detection of vimentin Ser phosphorylation by open-sandwich enzyme-linked immunosorbent assay (OS ELISA) with an anti-vimentin pSer71 antibody TM71 (Ohmuro-Matsuyama et al., 2012). In this assay, the interaction between the two antibody variable region domains, namely, V_H and V_L, was enhanced in the presence of phosphorylated peptide, which resulted in an increased absorbance signal. Only the target peptide was quantified with a wide working range, and non-phosphorylated peptide gave no signal increase. However, when the interaction between the V_H and V_L fragments was investigated by Förester resonance energy transfer (FRET) between them after their fluorolabeling, the change in FRET signal was not large enough to allow its quantification (data not shown).

As an alternative promising technology, recently we demonstrated a powerful antibody-based fluorescent biosensor strategy called Quenchbody (Abe et al., 2011). The Quenchbody works on the principle of antigen-dependent removal of quenching effect on a fluorophore that had been quenched by intrinsic tryptophan (Trp) residues of a single chain antibody variable region (scFv) (Fig. 1). This Quenchbody-based assay is superior to previous methods for the following points. First, it does not require any additional reagents to detect the target antigen but only needs Quenchbody itself, with some non-essential ingredients such as bovine serum albumin (BSA) and nonionic surfactant to protect the Quenchbody from non-specific adhesion to the cuvette. Second, the method is markedly rapid and simple, since it does not need either immobilization or washing steps but only needs adding the sample directly to the Quenchbody reagent to measure its fluorescence. Finally, the technology can be applied to the detection of a range of antigens from small haptens to large proteins with the same assay principle.

In this paper we describe the detection of vimentin phosphorylation at Ser71 (PS71) and Ser82 (PS82) based on the Quenchbody technology. PS71 and PS82 are important vimentin phosphorylation targets that occur during anaphase and metaphase of mitosis, respectively. First, we investigated new fluorescent dyes that can be incorporated for making Quenchbodies. In addition to carboxytetramethylrhodamine (TAMRA) used previously, two rhodamine dyes, rhodamine 6G (R6G) and ATTO 520 that share similar molecular structure were successfully incorporated to anti-BGP Quenchbody. The fluorescence intensity of the resultant Quenchbodies showed marked increases in an antigen concentration dependent way, suggesting their utility as a label of Quenchbody. Then we tried to detect PS71 and PS82 of vimentin with the corresponding Quenchbodies, and optimized reaction conditions as well as the Quenchbody structure itself. To the best of our knowledge, this study presents the first detection of protein serine phosphorylation with an antibody-based fluorescent biosensor.

2. Materials and methods

2.1. Materials

KOD-plus-neo DNA polymerase and In-Fusion advantage PCR cloning kit were from Takara Bio (Otsu, Japan). PureYield plasmid miniprep kit was from Promega (Tokyo, Japan). RYTS cell-free translation kit and dye-labeled tRNA were from ProteinExpress (Chiba, Japan). pROX-FL92.1amber harboring anti-BGP scFv gene was made as described (Abe et al., 2011). His Spin Trap column was from GE Healthcare (Piscataway, NJ). UltraFree-0.5 centrifugal device was from Millipore (Billerica, MA). C-terminal peptide from BGP (BGP-C7, NH_2-RRFYGPV-COOH, MW=894) was from Genscript (Piscaway, NJ). Vimentin peptides (PS71-containing peptide, CAVRLR(pS)SVPGV, MW=1323; S71-containing peptide, CAVRLRSSVPGV, MW=1243; PS82-containing peptide, RLLQD(pS)VDFSL, MW=1373; S82-containing peptide, RLLQDSVDFSL,

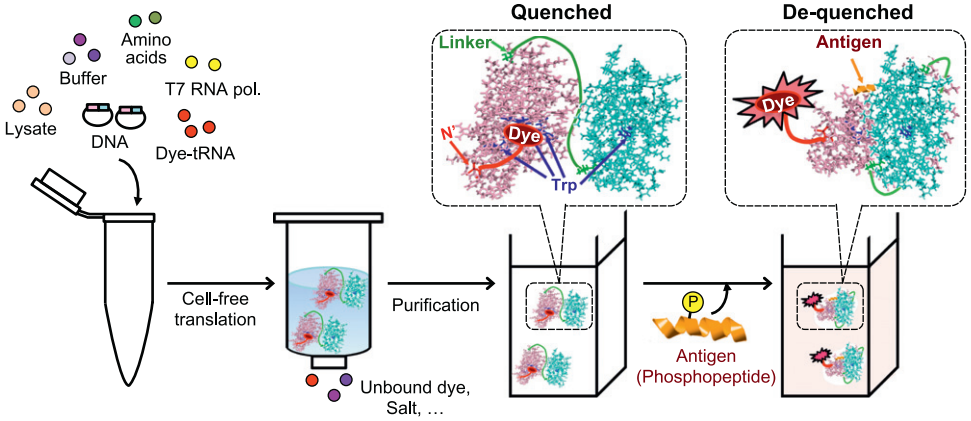

Fig. 1. Scheme of the Quenchbody assay for vimentin Ser phosphorylation.

MW=1293) were synthesized using the Fmoc solid-phase method and the fractions purified by semipreparative RP-HPLC were characterized by matrix-assisted laser desorption/ionization time-of-flight mass spectrometry. BSA was from Rockland (Philadelphia, USA). All the water used was purified with Milli-Q (Millipore).

2.2. Cloning of anti-phosphovimentin antibody Fv genes

The anti-PS71 and anti-PS82 scFv genes were cloned from the corresponding hybridoma TM71 and MO82, using Ig-Primer Sets (Novagen, Takara-Bio, Shiga, Japan). After that, the cloned V_H and V_L genes were each assembled by splice overlap extension (SOE) PCR with a $(G_4S)_3$ 15-amino acid linker inserted between them. The amplified scFv fragments were cloned into pTA2 (Takara-Bio), resulting in pTM71 and pMO82, respectively.

2.3. Construction of anti-phosphovimentin Quenchbody genes

A V_H-V_L type anti-PS71 scFv gene with N-terminal $(G_3S)_2$ and internal $(G_4S)_3$ linkers was amplified by PCR using primers TM71Back and VimFor (Table 1), pTM71 as a template, and KOD-plus-neo DNA polymerase. The PCR product was then inserted to *Nco*I- and *Sma*I-digested pROX-FL92.1amber plasmid using an In-Fusion PCR cloning kit, resulting in pROX-VLVHPS71. Using this plasmid as a template, another amber codon was incorporated to the middle of interdomain linker region by SOE PCR using primers TM71Back, LinkFor, AmbVLback, and VimFor (Table 1). The amplified gene was inserted to *Nco*I- and *Sma*I-digested pROX-FL92.1amber as above. The obtained plasmids were prepared with PureYield plasmid miniprep system, and confirmed the entire coding region sequences.

A V_H-$V_L$type anti-PS82 scFv gene with N-terminal $(G_3S)_2$ and internal $(G_4S)_3$ linkers was amplified by PCR using primers MO82Back and VimFor (Table 1), and pMO82 as a template, and inserted to *Nco*I- and *Sma*I-digested pROX-FL92.1amber as above, resulting in pROX-VLVHPS82. The gene was further used as a template of other types of anti-PS82 scFv genes as follow. A V_L-V_H type scFv gene was amplified by SOE PCR using primers MO82_VLVH_1, MO82_VLVH_2, MO82_VLVH_3, and MO82_VLVH_5, while another V_L-V_H type scFv gene incorporated with an additional amber codon in the middle of the interdomain linker was amplified with primers MO82_VLVH_1, MO82_VLVH_2, MO82_VLVH_4, and MO82_VLVH_5. Lastly, V_H-V_L type anti-PS82 scFv gene with an amber codon at the interdomain linker region was amplified with primers MO82Back, LinkFor, AmbVLback, and VimFor (Table 1). The constructed scFv genes were inserted to *Nco*I- and *Sma*I-digested pROX-FL92.1amber, and prepared with PureYield plasmid miniprep system, with their sequences confirmed for the entire coding region.

2.4. Cell-free protein synthesis

The synthesis of scFv position-specifically incorporated with fluorescence dye(s) was performed using an *E. coli* cell-free translation system (RYTS kit) according to the manufacturer. Briefly, the reaction mixture (50 μL) comprised of 16 μL of *E. coli* lysate, 0.5 μL of 150 mM methionine, 2.5 μL of enzyme mixture, 25 μL of reaction mixture, 150 ng of plasmid DNA, and 400 pmol of aminoacyl-tRNAs conjugated with either TAMRA, R6G, or ATTO520, was prepared and incubated for 2 h at 25 °C.

2.5. Purification

The full-length synthesized protein with C-terminal His-tag was subsequently purified with a His Spin Trap Column. First, the column was primed by 400 μL of wash buffer (20 mM phosphate, 0.5 M sodium chloride (NaCl), 60 mM imidazole, 0.1% polyoxyethylene(23)lauryl ether, pH 7.4). Then the reaction mixture, which was diluted in 350 μL of wash buffer, was applied to the column. After incubation at 25 °C for 15 min, the column was washed three times with 500 μL of wash buffer. Finally, the Quenchbody was eluted twice with 200 μL of elution buffer (20 mM phosphate, 0.5 M NaCl, 0.5 M imidazole, 0.1% polyoxyethylene(23)lauryl ether, pH 7.4). The eluent was subjected to an UltraFree-0.5 centrifugal device and equilibrated with PBST0.05 (0.05% Tween 20 in phosphate buffered saline, 10 mM phosphate, 137 mM NaCl, 2.7 m M potassium chloride, 0.05% Tween 20, pH 7.4) to exchange buffers. The concentration of buffer-exchanged Quenchbody was determined by comparing the fluorescence intensities of known concentrations of the dye and of the sample in 7 M guanidine hydrochloride, pH 7.4. The resultant Quenchbody reagent was dispensed at 2 μg/mL and stored at −80 °C.

2.6. Fluorescence measurements

To measure the fluorescence spectra, purified Quenchbody (2 μg/mL, 25 μL) was diluted in 200 μL of PBST0.05 containing 1% BSA, and antigen peptide was added by titration in a 5 × 5 mm quarts cell (GL Sciences, Tokyo, Japan). After each addition, the solution was incubated for 30 min at 25 °C prior to the spectral measurements. The fluorescence spectra were taken at 25 °C using a fluorescence spectrophotometer Model F-2500 (Hitachi High-technologies, Tokyo, Japan) with excitation at 546, 516 and 524 nm, for TAMRA, R6G, and ATTO520, respectively. Excitation and emission slit widths were set to 5.0 nm. Dose-response curves were fitted at the maximum emission wavelength using Kaleida Graph 4.1 (Synergy Software, Reading, PA).

Table 1
Nucleotide sequences of primers used in this study [a].

Primer name	Nucleotide sequence (5′–3′)
TM71Back	TCTAATGAGACCATGGGTGGCGGTTCAGGTGGCGGTTCACAGGTGAAACTGCAGCAG
VimFor	TGATGATGAGAACCCCCCCCCCGTTTCAGCTCCAGCTCCAGCTTGGT
MO82Back	TCTAATGAGACCATGGTGGCGGTTCAGGTGGCGGTTCAGAGGTGAAGCTGCAGGAG
MO82_VLVH_1	TCTAATGAGACCATGGGTGGCGGTTCAGGTGGCGGTTCACAGATCGTGTTGACCCAGTC
MO82_VLVH_2	GCCGCCGGAGCCGCCACCTCCACTCTCCAGCTCCAGCTTGGTCCCAGC
MO82_VLVH_3	GGCGGCTCCGGCGGCGGAGGTTCCGGAGGTGGTGGTTCAGAGGTGCAGCTGCAGGAGTCAGG
MO82_VLVH_4	GGCGGCTCCGGCGGCTAGGGATCCGGAGGTGGTGGTTCAGAGGTGCAGCTGCAGGAGTCAGG
MO82_VLVH_5	TGATGATGAGAACCCCCCCCTGAGGAGACGGTGACCGTGG
LinkFor	ACCACCGGAACCACCACC
AmbVLback	GGTGGTTCCGGTGGTTAGGGTTCCGGAGGTGGTGGTTCA

[a] The underline denotes the amber codon.

3. Results and discussion

3.1. Examination of rhodamine dyes as Quenchbody labels

As potential fluorescent dyes for making Quenchbodies, we tried to incorporate other rhodamine dyes (i.e., R6G and ATTO520) than TAMRA, which was successfully used in our previous study (Abe et al., 2011), into the N-terminal region of scFv to examine their utility. As a model scFv to evaluate these dyes, anti-human osteocalcin (bone gla protein, BGP) KTM219, which recognizes the C-terminus of the important biomarker for bone-related diseases (Lim et al., 2007) was used. We incorporated each dye into the N-terminal ProX tag region of the scFv using a cell-free transcription-translation system (Fig. 2A). After each Quenchbody was purified by nickel-affinity chromatography, its fluorescence spectra were measured in the presence of varied concentration of antigen BGP-C7 peptide. As a result, the fluorescence spectra of R6G- and ATTO520-labeled Quenchbodies showed remarkable BGP-C7 dose-dependent increases in intensity, as well as TAMRA-labeled Quenchbody (Fig. 2 B–D). The maximal fluorescence responses of TAMRA-, R6G-, and ATTO520-labeled Quenchbodies were 5.8-, 7.7-, and 2.9-fold, respectively. The fluorescence titration curves at their emission maxima clearly indicated BGP-C7 peptide concentration-dependent increase in fluorescence intensity (Supplementary Fig. S1). These results suggest that all these dyes were successfully incorporated into the scFv, and their quenching was removed in an antigen-dependent manner, suggesting these dyes as preferable labels of Quenchbody. Interestingly, the extent of fluorescence enhancement was different from dye to dye, which was caused by different extent of fluorescence quenching and its antigen-dependent release. Namely, the R6G-labeled Quenchbody showed superior response with deeper quenching than the others. Judged from their chemical structure (Supplementary Fig. S1, inset), R6G is more hydrophobic than TAMRA and ATTO 520. Indeed, a lipophilicity index (*Log P*) of R6G is reportedly higher (3.42) than that of TAMRA (2.9) (Ogawa et al., 2009). Therefore, the hydrophobicity of the dye is a possible important factor in the interaction between the fluorophore and Trp residues, which are scattered around hydrophobic V_H/V_L interface.

3.2. Binding activity of phosphovimentin Quenchbodies

Based on these results, we next tried to detect vimentin Ser phosphorylation by making specific Quenchbodies. Since the mechanism of Quenchbody is attributable to intramolecular quenching by highly conserved Trp residues in the variable region, we expected that we could make Quenchbodies using the two antibodies recognizing vimentin Ser phosphorylation, which also have a number of Trp residues in their variable region domains.

To this end, firstly we made two scFv expression vectors that target PS71 and PS82. After cell-free translation and purification of TAMRA-labeled Quenchbodies, the synthesized proteins were tested for their antigen binding activity by enzyme-linked immunosorbent assay (ELISA). The result of ELISA with immobilized BSA-peptide conjugates suggest that strong signals were observed for the wells with phosphorylated peptides, while much weaker signals were observed for the wells immobilized with non-phosphorylated peptides. Also, negligible signal was observed for the wells without peptide (Supplementary Fig. S2). The result clearly suggests that the binding specificity as well as the binding affinity of scFv for peptide was preserved even after incorporation of TAMRA dye into the N-terminal region of scFv.

3.3. Detection of vimentin Ser71 phosphorylation by Quenchbody

Next, we examined the detection of PS71 by Quenchbody. We incorporated TAMRA into the N-terminal region of the anti-PS71 scFv, which has four Trp residues (Fig. 3A), and then measured its fluorescence intensity in the absence and presence of the PS71 containing-peptide. As a result, the fluorescence intensity of TAMRA-labeled PS71 Quenchbody was increased when the PS71 containing-peptide was added (Fig. 3B). However, it was hardly changed when non-phosphorylated S71 peptide was added (Fig. 3C). The PS71 peptide dose-dependency curve showed 1.24 ± 0.06-fold increase of fluorescence intensity at the maximum emission wavelength (Fig. 3D). Interestingly, when PS71 peptide was added, the maximum of fluorescence peak shifted slightly to shorter wavelengths, indicating a blue shift of

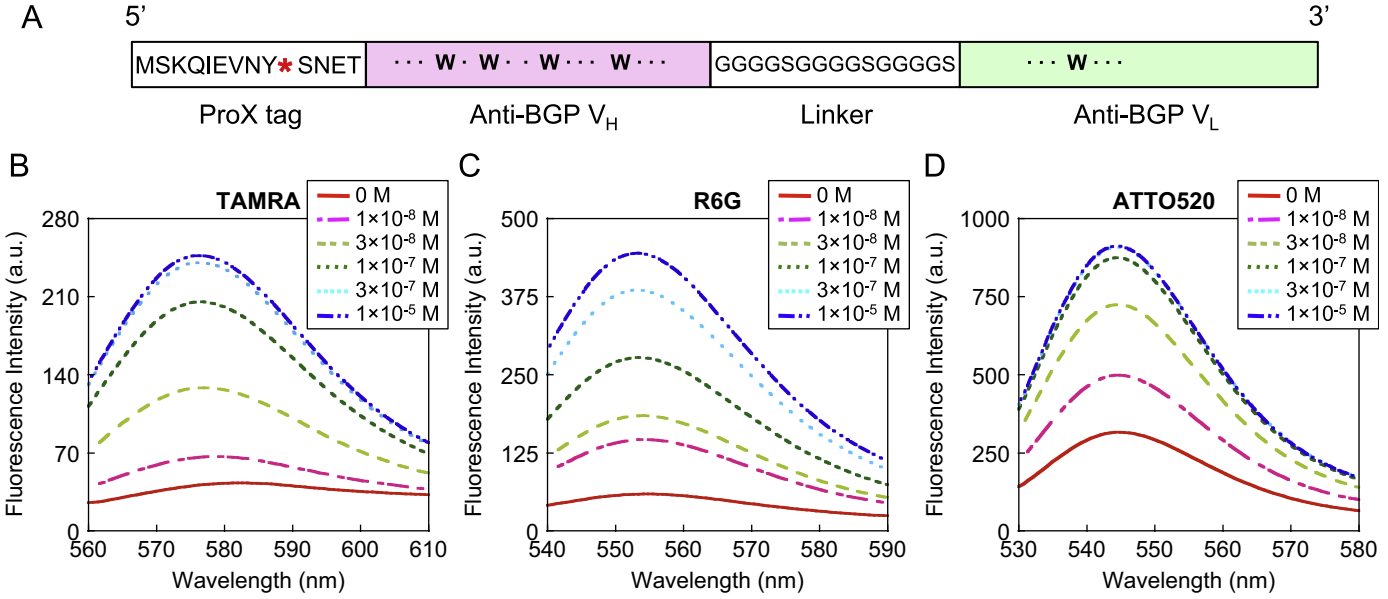

Fig. 2. Preparation of multicolor Quenchbodies. (A) Schematic representation of anti-BGP Quenchbody gene. Asterisk denotes the amber codon. (B–D) Fluorescence spectra of anti-BGP Quenchbodies in the presence of BGP-C7 at indicated concentrations. BGP-C7 was added by titration at 15 min intervals. TAMRA-labeled Quenchbody with excitation at 546 nm (B), R6G-labeled Quenchbody with excitation at 516 nm (C), and ATTO520-labeled Quenchbody with excitation at 524 nm (D) are shown.

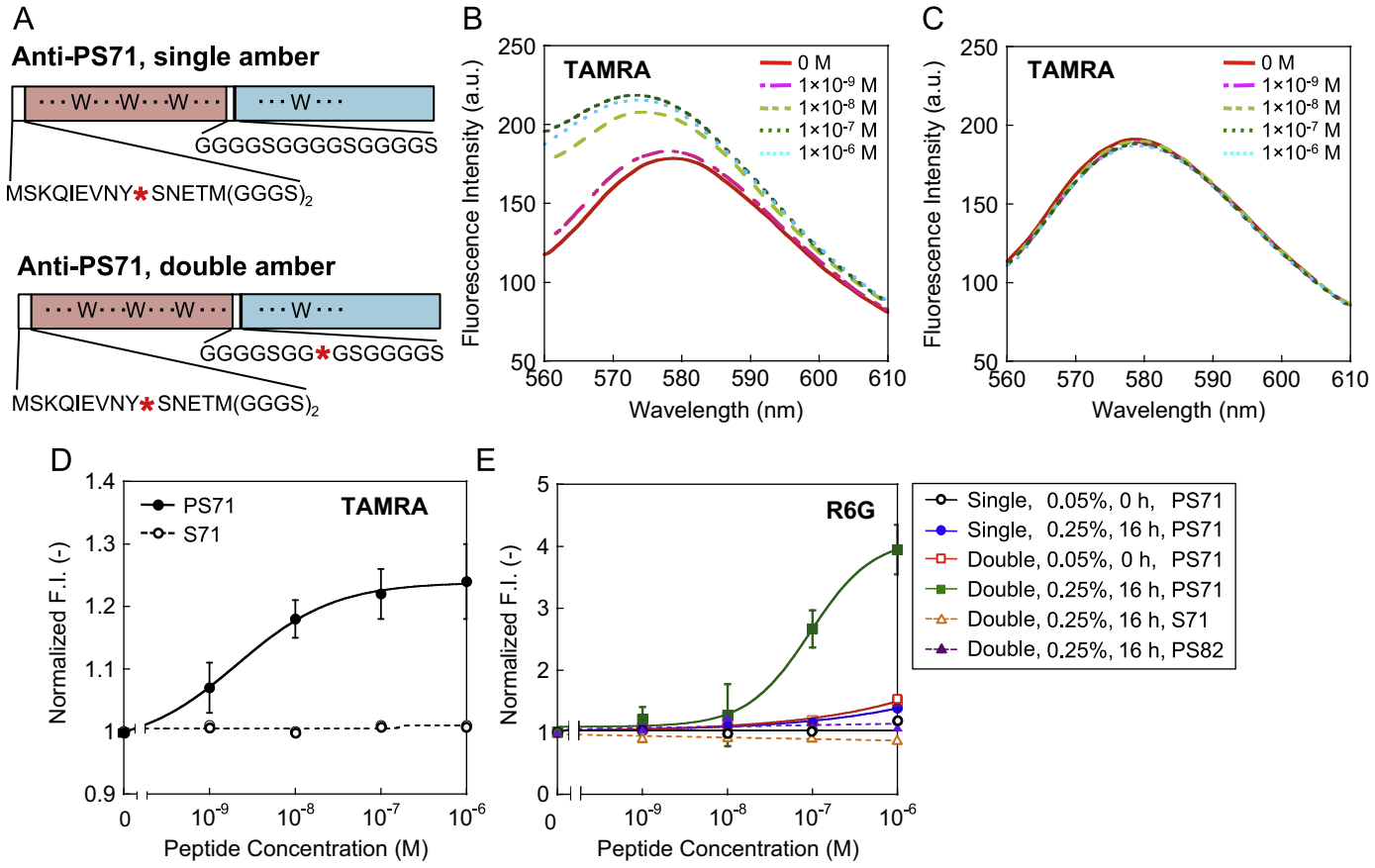

Fig. 3. (A) Schematic representations of PS71 Quenchbodies; asterisk denotes an amber codon. (B) Fluorescence spectra of TAMRA-labeled PS71 Quenchbody with excitation at 546 nm in the presence of PS71 peptide at indicated concentrations. (C) The same as in (B) except that S71 peptide was used. The peptides were added by titration at 30 min intervals. (D) Titration curves of the peak fluorescence intensity of TAMRA-labeled PS71 Quenchbody at 579 nm. RSD for PS71: 3.1% (n=10). (E) Titration curves of fluorescence intensity of R6G-labeled PS71 Quenchbodies at 553 nm; the percentage and the time denote the Tween 20 concentration and preincubation time, respectively. The normalized fluorescence intensity (F.I.) is the relative value with respect to that in the absence of antigen-peptide. RSD for Double, 0.25%, 16 h, PS71: 15.4% (n=15).

fluorescence emission. As the mechanism of antigen-dependent Quenchbody fluorescence, we inferred that the interaction between the fluorophore and Trp residues at the 'open state' contributed to fluorophore quenching by electron transfer processes. The binding of phosphorylated peptide to the Quenchbody will cause the closure of V_H/V_L interface, and subsequent exposure of otherwise quenched fluorophore to the outside of the protein will result in its de-quenching. In this 'closed' state, the polarity around the de-quenched fluorophore will be higher in the solvent (water), and the dye can possibly interact with the phosphate in the antigen and/or the buffer as a counter ion. Though further verification is needed, we think this might be the reason of the observed blue shift of fluorescence emission (Fujii et al., 2008; Kohn et al., 2000).

Although PS71 was detected with TAMRA-labeled Quenchbody, the obtained response was not satisfactory as a practical assay. Therefore, next we tried to label the Quenchbody with R6G, and also optimize the reaction buffer as well as the preincubation condition. Before optimization, PS71 peptide-dependent fluorescence of the Quenchbody was modestly improved to 1.27-fold by R6G-labeling instead of TAMRA-labeling (Fig. 3E, open circle). The higher fluorescence response for the R6G-labeled Quenchbody is similar to the case of the anti-BGP Quenchbody. Since we reasoned that the tendency of the dye to penetrate into hydrophobic V_H/V_L interface can be influenced by the surfactant (Tween 20) concentration and preincubation before antigen addition, several buffer and preincubation conditions were tested. After optimization of these conditions, the maximum fluorescence intensity was improved to 1.39-fold by increasing the Tween 20 concentration in the buffer to 0.25%, and by pre-incubating Quenchbody without sample for 16 h at 25 °C (Fig. 3E, filled circle). On the contrary, negligible changes were observed when the non-phosphorylated peptide was added (data not shown). Supposedly, the addition of optimal concentration (0.25%) of nonionic surfactant facilitates penetration of the fluorophore into the scFv, which results in deeper quenching and its antigen-dependent release. In addition, the unstable quenching state of Quenchbody was stabilized during this preincubation period. In other words, the 'open' state with the penetrated dye molecule might be stabilized by the preincubation, and resulted in more prominent antigen-induced de-quenching.

In addition, to attain further response by enhancing the quenching effect, we made another expression construct in which additional amber codon was incorporated to the middle of interdomain linker region as well as one in the N-terminal region, to incorporate two R6G molecules at these sites (Fig. 3A). The resultant doubly R6G-labeled Quenchbody at standard condition showed a slight fluorescence enhancement up to 1.51-fold (Fig. 3E, open square). Moreover, when we increased the Tween 20 concentration in the buffer to 0.25% and pre-incubated the Quenchbody for 16 h, the maximum fluorescence intensity was increased to 3.95 ± 0.4-fold (filled square), suggesting deeper quenching probably due to homo-dimerization (H-dimer formation) of the dyes (Ogawa et al., 2009) and its antigen-dependent release. At this condition, non-phosphorylated S71 peptide (open triangle) and non-cognate PS82 peptide (filled triangle) showed

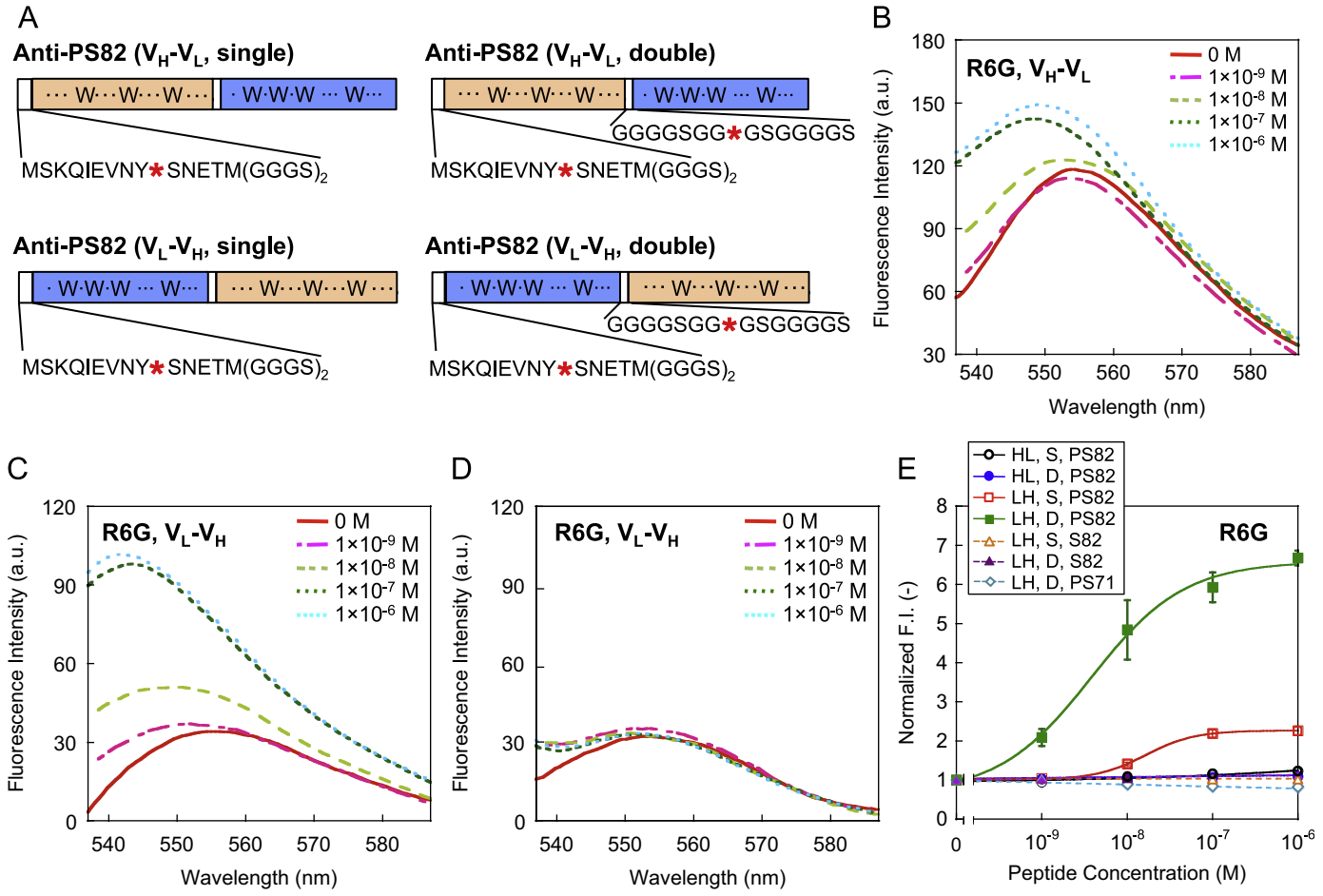

Fig. 4. (A) Schematic representations of PS82 Quenchbodies; asterisk denotes an amber codon. (B) Fluorescence spectra of R6G-labeled V_H-V_L type PS82 Quenchbody with excitation at 516 nm in the presence of PS82 peptide at indicated concentrations. (C) Fluorescence spectra of R6G-labeled V_L-V_H type PS82 Quenchbody with excitation at 516 nm in the presence of PS82 peptide. (D) The same as in (C) except that S82 peptide was used. The peptides were added by titration at 30 min intervals. (E) Fluorescence titration curves of R6G-labeled PS82 Quenchbodies at 553 nm; HL, LH, single, double, PS and S denote V_H-V_L type, V_L-V_H type, one amber codon, double amber codons, PS82 peptide and S82 peptide, respectively. RSD for LH, D, PS82: 7.1% (n=15).

negligible signals, showing its detection specificity. These results suggest that the fluorescence response is also influenced by the number of R6G dyes incorporated in a Quenchbody.

3.4. Detection of vimentin Ser82 phosphorylation by Quenchbody

Next we tried to detect another vimentin phosphorylation at Ser82 (PS82) with the Quenchbodies. When we incorporated R6G into the N-terminal region of the anti-PS82 scFv (V_H-V_L) (Fig. 4A) and compared its fluorescence intensities in the absence and presence of PS82-containing peptide, the intensity showed modest increase of 1.23-fold (Fig. 4B). In view of increasing this response, we made another Quenchbody in which the orientation of V_H and V_L domains are reversed to V_L-V_H. This was partly because there are more Trp residues (four) in the V_L domain than in the V_H domain (three) of this antibody, and the dye attached to V_L might have higher chance of quenching. Also, in view of attaining further response, we made a series of constructs in which another amber codon was incorporated to the middle of interdomain linker region, to incorporate two R6G molecules (Fig. 4A). Although the optimization of reaction condition was also possible, considering the practical utility, standard condition (0.05% Tween 20 in PBS without preincubation) was employed.

As a result, the fluorescence intensity of mono R6G-labeled V_L-V_H type Quenchbody at the maximum emission wavelength of R6G (553 nm) was increased to 2.15 ± 0.01-fold when added with PS82-containing peptide, while it was hardly changed upon addition of non-phosphorylated peptide (Fig. 4C–E, open square and open triangle). Moreover, as seen in Fig. 4C, in this case not only higher intensity enhancement but also larger blue shift was observed than the V_H-V_L type Quenchbody.

When we prepared and used multilabeled Quenchbodies for the fluorescence measurement, we found that the doubly R6G-labeled V_L-V_H type Quenchbody showed a significant fluorescence enhancement up to 6.7 ± 0.2-fold, suggesting deeper quenching probably due to homo-dimerization (H-dimer formation) of the dyes (Fig. 4E, filled square). On the contrary, negligible fluorescence enhancement was observed when the non-phosphorylated S82 peptide (filled triangle) or PS71 peptide (open diamond) was added. These results suggest that the fluorescence response is influenced not only by the number of dyes but also the configuration of scFv molecule. The response of doubly R6G-labeled V_L-V_H type Quenchbody was observed with subpicomole amount of PS82-containing peptide, with its EC_{50} value estimated as 3.8×10^{-9} M, indicating the high sensitivity of this Quenchbody-based protein phosphorylation biosensor.

4. Conclusions

Here we report several extensions of previously demonstrated Quenchbody-based technology. First, incorporation of not only

TAMRA but also R6G and ATTO520 into the N-terminal region of anti-BGP scFv resulted in significant antigen-dependent fluorescence response, showing the possibility of multicolor measurement by using these dyes. It is worth noting that the response of R6G-labeled Quenchbody was similar or superior to corresponding TAMRA-labeled ones, suggesting the usefulness of R6G dye as a preferred label of Quenchbody. Second, we could utilize Quenchbody for the specific detection of vimentin Ser phosphorylation at their two locations. The maximal responses of PS71 and PS82 Quenchbody were 4.0- and 6.7-fold, respectively, whereas negligible changes were observed upon addition of non-phosphorylated or non-target peptides. Thirdly, as a result of assay optimization we could observe positive effect of surfactant Tween 20 concentration and longer preincubation for the response. However, the attainable response was case-by-case depending on the antibody, probably reflecting its number and the position of the Trp residues.

Finally, the effect of double labeling was shown to enhance its response, probably due to deeper quenching in the absence of antigen due to H-dimer formation between the dyes. Rhodamine derivatives form homodimers called H-dimers at relatively high concentrations, and the photophysical chemistry underlying quenching by dimerization in concentrated aqueous solutions has been well studied (Kemnitz and Yoshihara, 1991; Lopez Arbeloa and Ruiz Ojeda, 1982). The H-dimer of rhodamines induces blue shifts of absorbance spectra, which completely quench the fluorescence emission (Ogawa et al., 2009; Valdes-Aguilera and Neckers, 1989). In our case, since the presumptive H-dimer-induced quenching of double-labeled Quenchbodies was found effectively released by antigen addition, this will be a general method to improve the responses of other Quenchbodies with modest signal enhancements.

Taken together, this Quenchbody-based phosphorylation biosensor will afford a valuable approach to the precise and reliable clinical diagnostics with rapid, simple and high-sensitive manner. In addition to its application to in vitro screening, the constructed Quenchbody probes will have a utility for live cell imaging, since only the probe that binds to the phosphorylated target shows bright fluorescence. Through the combination of multicolor probes for several targets, the Quenchbody technology will further expand its fertile world of biosensing and bioimaging.

Acknowledgments

We thank Tatsuya Shinoda for allowing the use of anti-BGP gene, and Ryoji Abe and Hiroaki Takagi for valuable suggestions. This work was supported by Grant-in-Aid for Scientific Research on Priority Areas (525) from MEXT, Japan, by Grant-in-Aid for Challenging Exploratory Research (23656517) from JSPS, Japan, and by the Global COE Program for Chemistry Innovation, MEXT, Japan.

Appendix A. Supplementary information

Supplementary data associated with this article can be found in the online version at http://dx.doi.org/10.1016/j.bios.2012.06.030.

References

Abe, R., Ohashi, H., Iijima, I., Ihara, M., Takagi, H., Hohsaka, T., Ueda, H., 2011. Journal of the American Chemical Society 133, 17386–17394.
Aziz, A., Hess, J.F., Budamagunta, M.S., Voss, J.C., Fitzgerald, P.G., 2010. The Journal of Biological Chemistry 285, 15278–15285.
Bouamrani, A., Ramus, C., Gay, E., Pelletier, L., Cubizolles, M., Brugiere, S., Wion, D., Berger, F., Issartel, J.P., 2010. PLoS One 5, e9238.
Brune, M., Corrie, J.E., Webb, M.R., 2001. Biochemistry 40, 5087–5094.
Chang, I.A., Oh, M.J., Kim, M.H., Park, S.K., Kim, B.G., Namgung, U., 2012. FASEB Journal.
Cotton, G.J., Muir, T.W., 2000. Chemistry and Biology 7, 253–261.
Fujii, K., Iyi, N., Sasai, R., Hayashi, S., 2008. Chemistry of Materials 20, 2994–3002.
Goto, H., Inagaki, M., 2007. Nature Protocols 2, 2574–2581.
Graves, J.D., Krebs, E.G., 1999. Pharmacology and Therapeutics 82, 111–121.
Holford, T.R., Davis, F., Higson, S.P., 2012. Biosensors and Bioelectron 34, 12–24.
Inagaki, M., Nishi, Y., Nishizawa, K., Matsuyama, M., Sato, C., 1987. Nature 328, 649–652.
Ivaska, J., Pallari, H.M., Nevo, J., Eriksson, J.E., 2007. Experimental Cell Research 313, 2050–2062.
Izawa, I., Inagaki, M., 2006. Cancer Science 97, 167–174.
Kawai, Y., Sato, M., Umezawa, Y., 2004. Analytical Chemistry 76, 6144–6149.
Kemnitz, K., Yoshihara, K., 1991. Journal of Physical Chemistry 95, 6095–6104.
Kohn, F., Hofkens, J., De Schryver, F.C., 2000. Chemical Physics Letters 321, 372–378.
Lawrence, D.S., Wang, Q., 2007. Chembiochem 8, 373–378.
Lee, K.Y., Liu, L., Jin, Y., Fu, S.B., Rosales, J.L., 2011. Journal of Cell Physiology 227, 739–750.
Lim, S.L., Ichinose, H., Shinoda, T., Ueda, H., 2007. Analytical Chemistry 79, 6193–6200.
Lopez Arbeloa, I., Ruiz Ojeda, P., 1982. Chemical Physics Letters 87, 556–560.
Marks, F., 2001. Journal of Cancer Research and Clinical Oncology 127, 744–750.
Minin, A.A., Moldaver, M.V., 2008. Biochemistry (Mosc) 73, 1453–1466.
Mundy, J., Schneitz, K., 2002. Trends in Plant Science 7, 54–55.
Ogawa, M., Kosaka, N., Choyke, P.L., Kobayashi, H., 2009. ACS Chemical Biology 4, 535–546.
Ohmuro-Matsuyama, Y., Inagaki, M., Ueda, H., 2012. Detection of Protein-Phosphorylation by Open-Sandwich Immunoassay. In: Leung, H.-C. (Ed.), Integrative Proteomics.. InTech, Rijeka, Croatia.
Pittenger, J.T., Hess, J.F., Budamagunta, M.S., Voss, J.C., Fitzgerald, P.G., 2008. Biochemistry 47, 10863–10870.
Sawyer, T.K., Shakespeare, W.C., Wang, Y., Sundaramoorthi, R., Huang, W.S., Metcalf 3rd, C.A., Thomas, M., Lawrence, B.M., Rozamus, L., Noehre, J., Zhu, X., Narula, S., Bohacek, R.S., Weigele, M., Dalgarno, D.C., 2005. Medicinal Chemistry 1, 293–319.
Sihag, R.K., Inagaki, M., Yamaguchi, T., Shea, T.B., Pant, H.C., 2007. Experimental Cell Research 313, 2098–2109.
Takai, Y., Ogawara, M., Tomono, Y., Moritoh, C., Imajoh-Ohmi, S., Tsutsumi, O., Taketani, Y., Inagaki, M., 1996. Journal of Cell Biology 133, 141–149.
Thaiparambil, J.T., Bender, L., Ganesh, T., Kline, E., Patel, P., Liu, Y., Tighiouart, M., Vertino, P.M., Harvey, R.D., Garcia, A., Marcus, A.I., 2011. International Journal of Cancer 129, 2744–2755.
Valdes-Aguilera, O., Neckers, D.C., 1989. Accounts of Chemical Research 22, 171–177.